Spontaneous emission in cavity QED with a terminated waveguide

Matthew Bradford* and Jung-Tsung Shen†

Department of Electrical and Systems Engineering, Washington University in St. Louis, St. Louis, Missouri 63130, USA

(Received 14 March 2013; revised manuscript received 15 May 2013; published 19 June 2013)

We investigate the effects of a nanophotonic boundary on the spontaneous emission properties of an excited two-level atom in cavity quantum electrodynamics (QED) geometry. We show that a boundary provides temporally delayed interference, which can be either constructive or destructive. Consequently, the decay of the atomic excitation can be either increased or greatly inhibited. As a concrete example, we investigate the spontaneous emission process in cavity QED with a terminated line-defect waveguide, and show the rich behavior of the atomic response due to the boundary. We also show that the output photonic wave form is strongly influenced by the boundary.

DOI: 10.1103/PhysRevA.87.063830 PACS number(s): 42.50.Pq, 42.79.Gn

I. INTRODUCTION

The field of quantum nanophotonics has recently attracted considerable interest. In quantum nanophotonics, fermionic degrees of freedom are coupled to bosonic degrees of freedom. As the fermionic components can be saturated by a finite number of photons, the interplay between the two degrees of freedom can fundamentally alter the transport properties of photons and their correlations. A fermionic component can be a quantum dot [1,2], a superconducting qubit [3,4], or an atom [5,6], and is hereafter referred to simply as an "atom." By coupling photons to an atom in a waveguide [waveguide quantum electrodynamics (QED)] [7,8] or in a microcavity (cavity QED) [9–11], strong atom-photon and photon-photon interactions can be created. For example, a two-level atom in a waveguide can completely reflect a resonant photon [12]; it can also induce photon-photon interaction and create a two-photon bound state [13]. Moreover, a photon blockade, wherein atomic excitation due to one photon blocks the transmission of a subsequent photon, has been demonstrated with a single atom coupled to an optical cavity [14]. The influence of a cavity on spontaneous emission has also been investigated [15].

On a separate front, it has been recognized that the specific properties of the reservoir can affect the atomic decay rate and therefore provide a route to counteract or control spontaneous emission by engineering the reservoir. In particular, the effects of a boundary close to an emitter are well known. For example, the radiation patterns of an antenna in front of a metallic plate can be significantly modified depending on the distance from the plate [16]. The interference of radiation from an ion near a mirror and its mirror image has also been confirmed [5]. In quantum nanophotonics, there have been important recent experimental developments making use of a boundary for dynamic control of photons [17], for bright single-photon sources [18], and for enhancing photon emission efficiency in nanowires [19]. Recently, the effects of a variable boundary on the dynamics of a superconducting qubit have been studied using input-output formalism [20]. The effects of a mirror on spontaneous emission have also been investigated [21,22].

Nonetheless, the full capability of controlling the atomic and photonic degrees of freedom in quantum nanophotonics by engineering the reservoir has not been thoroughly explored. In this paper, we investigate the atomic response and photonic dynamics in cavity QED with a terminated waveguide. By introducing a boundary to reflect photons back to the system, the boundary provides a mechanism for temporally delayed feedback interference. The boundary could be a physical end of the waveguide or a heterogeneous interface, including terminated photonic line-defect waveguides, nanowires, and the capacitative gaps in microwave transmission lines in circuit QED. The photonic density of states and the dispersion relations across the boundary could change substantially to have a direct impact on the transport properties. As a result, the transport properties and the correlations between photons, the output photonic wave forms, and the temporal response of the atom exhibit completely different characteristics and can be controlled by boundary and dispersion engineering.

In particular, we show that the temporal behavior of the excited atom can be qualitatively modified: Following a very short period of free decay, the boundary can enhance or suppress the atomic decay rate by orders of magnitude. Accordingly, the temporal duration of the emitted photons can be narrowed or broadened, allowing applications in single-photon wave form engineering [23,24]. We also show that the scheme is effective by providing a realistic estimate using parameters from experiments.

The paper is organized as follows. In Sec. II, we discuss spontaneous emission with a bi-infinite waveguide for both waveguide and cavity quantum electrodynamics (waveguide and cavity QED) geometries. In Sec. III, we discuss spontaneous emission in the presence of a boundary. We begin by providing physical intuition for the feedback interference provided by a boundary and its effects on the spontaneous emission process. We then describe several physical realizations of a boundary and their optical properties. Next we present a general theoretical framework to study spontaneous emission with a boundary. Using this framework, we investigate the temporal behavior of the atomic excitation and emitted photonic wave packets and compare these to the case of a bi-infinite waveguide. We then discuss the effects of dissipation on the process. In Sec. IV we provide our outlook and discuss possibilities for future expansion. The results of waveguide and cavity QED for cases with and without boundaries are presented in parallel for comparison. Finally,

*bradfordm@ese.wustl.edu
†jushen@ese.wustl.edu

in the Appendix we provide detailed calculations for the results presented in the paper.

II. SPONTANEOUS EMISSION INTO A BI-INFINITE WAVEGUIDE

In this paper we consider spontaneous emission in waveguide QED [Fig. 1(a)] and cavity QED [Fig. 1(b)] geometries. Such configurations have been extensively explored in quantum nanophotonics. In either case, the coupling of the atom to the bi-infinite waveguide is regarded as a loss mechanism for the atom and always gives rise to an irreversible decay of the atomic excitation. Here we highlight the physics of the spontaneous emission process and assume no other intrinsic dissipation mechanism for the atom, where intrinsic dissipation refers to the loss mechanism of a photon to any nonwaveguided channel. The effects of intrinsic dissipation are discussed in the Appendix.

A. Waveguide QED

When an excited atom is coupled to the vacuum of the radiation field, the atom will undergo spontaneous emission (Weisskopf-Wigner decay). That is, the atom will relax to its ground state and emit a photon. The atomic excitation is described by

$$\dot{e}_2(t) + g_0 e_2(t) = 0, \tag{1}$$

where $e_2(t)$ is the atomic excitation amplitude at time t and g_0 is the radiative decay rate [25,26]. Equation (1) describes exponential decay $e_2(t) \propto e^{-g_0 t}$, which is characterized by a single time scale $1/g_0$. It is likewise well known that when an excited atom couples to a bi-infinite waveguide in waveguide QED geometry [Fig. 1(a)], the atom will also spontaneously decay, and the atomic excitation obeys the same form.

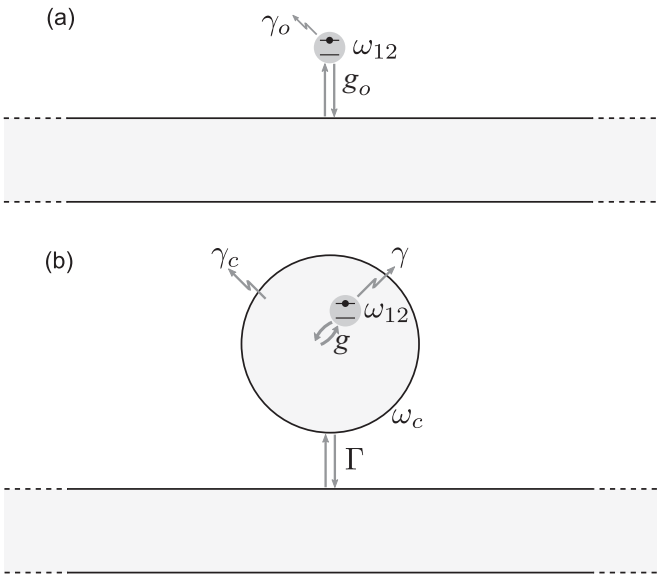

FIG. 1. Atom coupled to a bi-infinite waveguide. (a) Waveguide QED. (b) Cavity QED.

B. Cavity QED

The short-term atomic decay can be modified by coupling the atom to a cavity, as in cavity QED [Fig. 1(b)]. As the atom relaxes to its ground state, cavity modes can reexcite the atom, which leads to coherent energy exchange between the cavity and the atom. Coupling to the waveguide manifests as a loss mechanism to this process. As a result, the excitation obeys a damped harmonic oscillator equation [27]

$$\ddot{e}_2(t) + (\Gamma + i\Delta)\dot{e}_2(t) + g^2 e_2(t) = 0, \tag{2}$$

where g is the atom-cavity coupling strength, Γ is the cavity-waveguide coupling strength, and $\Delta = \omega_c - \omega_{12}$ is the cavity-atom frequency detuning. The atomic excitation can undergo decaying oscillations in the underdamped case ($\Gamma < 2g$) or monotonic decay in the overdamped case ($\Gamma > 2g$). The long-time behavior still exhibits exponential decay.

For both of the cases shown in Fig. 1, the critical feature is that the spontaneously emitted wave always leaks into the waveguide. This leakage, however, can be slowed by, for example, introducing interference via a feedback mechanism. In particular, we show that by using a boundary, the time scale

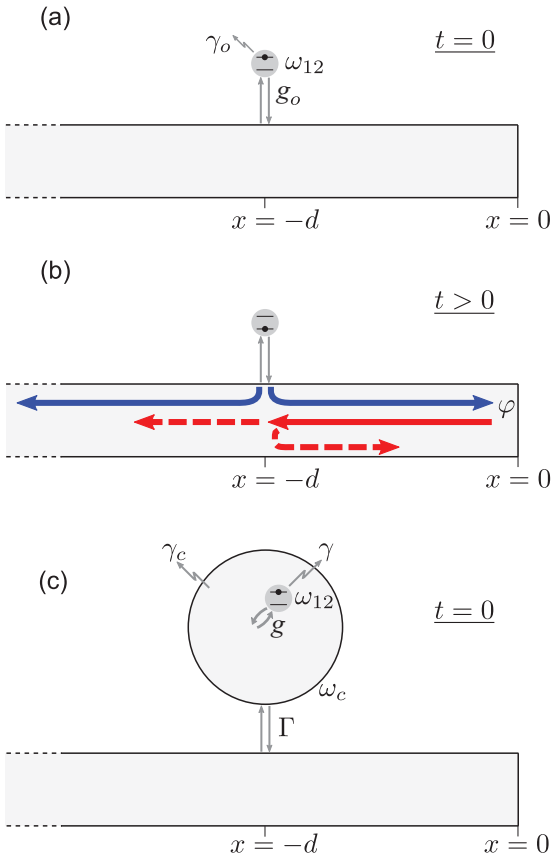

FIG. 2. (Color online) Atom coupled to a terminated waveguide. (a) Initial state in waveguide QED. At $t = 0$, the atom is excited. (b) At $t > 0$, the atom relaxes to its ground state and spontaneously emits into the waveguide. Blue arrows indicate initial, unperturbed emitted waves. Solid red arrows indicate the photonic modes reflected by the boundary, which obtain an additional phase φ. The reflection is then partially transmitted and partially reflected (dashed red arrows) due to coupling with the atom. The secondary reflected wave repeats the process, providing further feedback. (c) Cavity QED case.

of the spontaneous emission process can be much longer than for the case of a bi-infinite waveguide.

III. SPONTANEOUS EMISSION INTO A SEMI-INFINITE WAVEGUIDE WITH A BOUNDARY

The presence of a boundary provides a delayed feedback mechanism to modify the temporal behavior of the spontaneous emission process. By terminating one end of a bi-infinite waveguide, a boundary can be formed to reflect photons [Fig. 2] and generate interference. To illustrate the physics, we first consider the waveguide QED case in Fig. 2(a). As the atom decays, it will excite both left- and right-moving waveguided modes [shown in solid blue in Fig. 2]. When the right-moving waves are reflected by the boundary, they acquire a reflection phase φ in addition to the propagation phase. The reflected modes (solid red) are subsequently absorbed or scattered by the atom, giving rise to secondary transmitted and reflected modes (dashed red). The secondary reflected modes return to the boundary and repeat the process. The contributions of all transmitted waves interfere with the initial left-moving wave. Consequently, the spontaneous decay rate can be greatly enhanced for constructive interference or largely suppressed for destructive interference.

In the same fashion, spontaneous emission in cavity QED can be fundamentally altered by including a boundary as in Fig. 2(c). The boundary will provide a feedback channel analogous to that shown in Fig. 2(b).

Photonic boundaries which can reflect photonic modes can be formed in many nanophotonic configurations, ranging from optical [17] to microwave [20,28] frequency regimes. In the following section, we describe boundary implementations in several important systems and discuss the resulting reflection phase.

A. Boundary implementations

One important physical realization of a boundary is a terminated line-defect waveguide in photonic crystal as shown in Fig. 3(a), which is formed by removing half a line of air holes from an otherwise perfect triangular lattice of air holes in silicon. Such terminated line-defect waveguides have been both theoretically investigated and experimentally realized in quantum nanophotonics [17].

Figure 3(b) shows the band diagram for the perfect crystal, which has a complete band gap over the range $0.4 < fa/c < 0.44$, where a is the lattice constant. As shown in Fig. 3(c), the terminated line-defect waveguide introduces transverse electric (TE) and transverse magnetic (TM) defect bands within the band gap. Within a wide frequency range, the terminated waveguide is a single-polarization-single-mode (SPSM) waveguide with essentially linear dispersion for the TE defect mode. We note that an SPSM waveguide is crucial to the operation of the device, as mode conversion deteriorates interference effects.

When photons are reflected by the boundary, they acquire a reflection phase φ which, in general, can be a function of

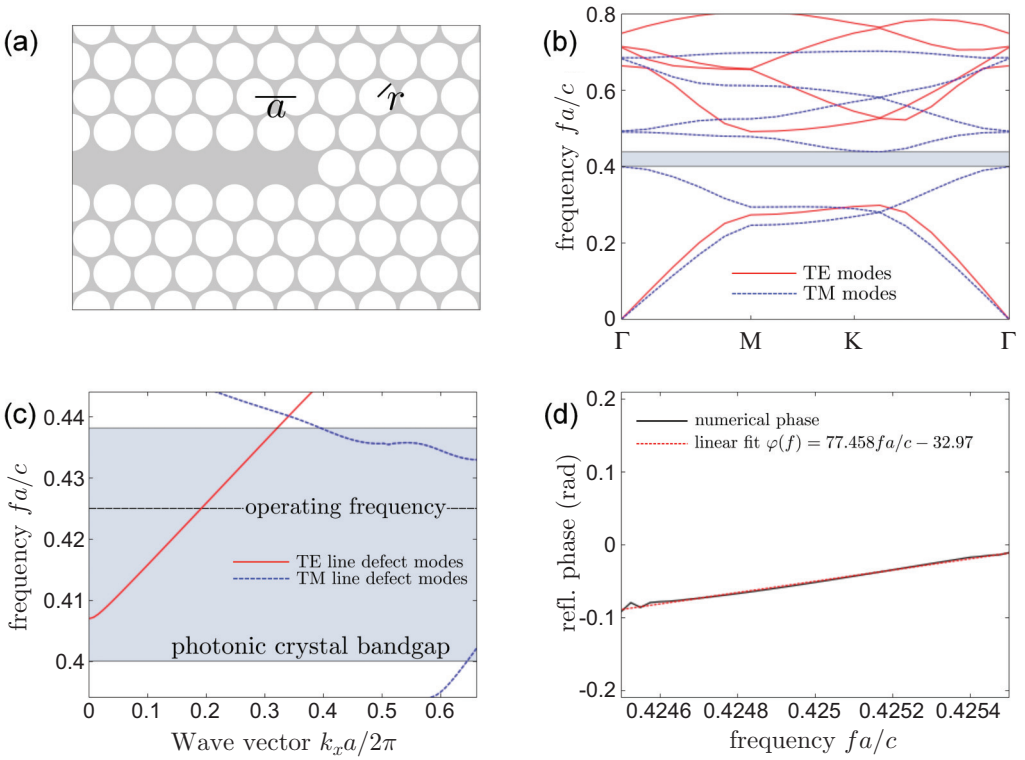

FIG. 3. (Color online) Photonic crystal realization of a terminated waveguide. (a) The terminated waveguide is formed by a line defect in a triangular lattice of air holes in silicon ($\epsilon_r = 12.1$) [29] with lattice constant a and $r = 0.45a$. (b) The perfect crystal has a complete photonic band gap shown in gray. (c) A TE defect mode arises when a line defect is introduced, forming an SPSM waveguide at the operating frequency, where $v_g = c/9.89$. A TM defect mode is also found. (d) The reflection phase due to the boundary is nearly constant over the bandwidth of interest.

frequency. We found numerically that in the frequency range where the dispersion is linear, the phase is linear in frequency and can be described by

$$\varphi(fa/c) = 77.458\, fa/c - 32.970. \tag{3}$$

Figure 3(d) plots the reflection phase for the frequency range $0.4245 < fa/c < 0.4255$.

For $fa/c = 0.425$ and an operating wavelength $\lambda = 1.55\ \mu$m, the lattice constant is given by $a = 0.659\ \mu$m. For a realistic photonic pulse with 1 GHz bandwidth, the reflection phase change is $O(10^{-4})$, which is essentially constant. Consequently, discussions in the following sections assume a frequency independent reflection phase φ.

Other important physical realizations of a photonic boundary include a fiber Bragg grating [30], the tapered region of a tapered waveguide [31], or a capacitive gap in a superconducting microwave transmission line [20,28]. In fiber Bragg grating or tapered waveguide geometries, each frequency component of the incoming photonic pulse is reflected at a different spatial point, yielding a different round-trip path length for each component. As a result, the reflection phase is strongly frequency dependent and can be controlled by the geometry of the waveguide. Finally, in circuit QED, a SQUID ring at the end of a microwave transmission line acts as a boundary and can be used to control the reflection phase [20].

Further control of the emission process can be obtained through dynamic control of the reflection phase. In photonic crystal geometry, this can be achieved by modulating the refractive index at the boundary, while in circuit QED, one can modulate the SQUID ring with a time-varying magnetic field.

B. Theoretical framework

There have been different approaches to model a boundary. For example, in condensed matter physics, a chiral description using unfolding techniques has been developed [32–34]. This chiral description has also been employed in photonic systems [35]. The chiral description, while mathematically equivalent, describes the situation wherein photons flow unidirectionally and never get reflected. Here, instead of employing unfolding techniques, we describe the physical geometry directly. Our formalism incorporates the physical action of the boundary on the photonic modes in the terminated waveguide. By including the boundary term in the Hamiltonian, we obtain the equations of motion that describe the full spatiotemporal dynamics of the scattering process. We have found numerically that our method and unfolding techniques are equivalent.

1. Waveguide QED

In waveguide QED geometry [Fig. 2(a)], the total system Hamiltonian is

$$H = H_w + H_a + H_i + H_b. \tag{4}$$

H_w is the free Hamiltonian of photons propagating in the terminated waveguide and is given by

$$H_w = \hbar \int_{-\infty}^{0} dx \left\{ c_R^\dagger(x)(-i v_g \partial_x) c_R(x) + c_L^\dagger(x)(i v_g \partial_x) c_L(x) \right\}, \tag{5}$$

where we integrate over the semi-infinite waveguide from $x = -\infty$ to $x = 0$. Here, $c_R^\dagger(x)$ and $c_R(x)$ are creation and annihilation operators for a right-moving photon at position x, $c_L^\dagger(x)$ and $c_L(x)$ are creation and annihilation operators for a left-moving photon at position x, and v_g is the group velocity of photons in the waveguide. Such a photonic Hamiltonian for the case of a bi-infinite waveguide has been previously investigated [12].

H_a is the Hamiltonian for the atom and is given by

$$H_a = \hbar\omega_1 a_1^\dagger a_1 + \hbar\omega_2 a_2^\dagger a_2, \tag{6}$$

where $a_i^\dagger$ and a_i are creation and annihilation operators for the ith atomic state, which satisfy standard fermionic anticommutation relations; and $\hbar\omega_1$ and $\hbar\omega_2$ are the energies of the atomic ground state $|1\rangle$ and excited state $|2\rangle$, respectively. We note that in quantum optics and atomic physics, a two-level atom is usually described in terms of Pauli spin operators. An equivalent atomic Hamiltonian using Pauli spin operators is presented in the Appendix.

H_i describes the interaction between guided photonic modes and the atom and is given by

$$H_i = \hbar \int_{-\infty}^{0} dx\, V\delta(x+d)\big[c_R^\dagger(x)a_1^\dagger a_2 + c_L^\dagger(x)a_1^\dagger a_2 + a_2^\dagger a_1 c_R(x) + a_2^\dagger a_1 c_L(x)\big], \tag{7}$$

where V is the coupling strength between the atom and the photonic field in the waveguide. H_i describes all emission and absorption processes between the atom and photons. For example, the term proportional to $c_R^\dagger(x)a_1^\dagger a_2$ describes an atomic transition from the excited $|2\rangle$ state to the $|1\rangle$ ground state and the spontaneous emission of a right-moving photon.

H_b describes the action of the boundary on photonic modes and is given by

$$H_b = \hbar \int_{-\infty}^{0^+} dx\, \delta(x)\big[i2v_g e^{i\varphi} c_L^\dagger(-x) c_R(x) - i2v_g e^{-i\varphi} c_R^\dagger(-x) c_L(x)\big]. \tag{8}$$

Here, the boundary is located at $x = 0$ and the first term describes the event that an incoming right-moving photon is reflected into a left-moving outgoing photon and acquires a phase φ, while the second term ensures that the Hamiltonian is Hermitian. The validity of the boundary term is established in the Appendix.

The Hamiltonian in Eq. (4) is general and is applicable to a state with an arbitrary number of photons. Here we restrict ourselves to one-photon processes, which includes spontaneous emission. The general one-photon state of the system is

$$|\psi\rangle = \int_{-\infty}^{0} dx\, \phi_R(x,t) e^{-i\omega_1 t} c_R^\dagger(x) a_1^\dagger |0\rangle + \int_{-\infty}^{0} dx\, \phi_L(x,t) e^{-i\omega_1 t} c_L^\dagger(x) a_1^\dagger |0\rangle + e_2(t) e^{-i\omega_2 t} a_2^\dagger |0\rangle, \tag{9}$$

where $\phi_R(x,t)$ and $\phi_L(x,t)$ are amplitudes of right- and left-moving photonic modes in the waveguide and $e_2(t)$ is the

excitation amplitude of the atom. In Eq. (9), the phase due to the temporal evolution of the atomic states ($e^{-i\omega_1 t}$ and $e^{-i\omega_2 t}$) is written explicitly for convenience, so that $\phi_R(x,t)$ and $\phi_L(x,t)$ contain only the temporal response of the photons.

Solving the Schrödinger equation $i\hbar\partial_t|\psi\rangle = H|\psi\rangle$ with the given Hamiltonian and state yields the equations of motion

$$\begin{aligned} i\partial_t\phi_R(x,t) &= -iv_g\partial_x\phi_R(x,t) - i2v_g e^{-i\varphi}\phi_L(-x,t)\delta(x) \\ &\quad + V\delta(x+d)e_2(t)e^{-i\omega_{12}t}, \qquad (10a) \\ i\partial_t\phi_L(x,t) &= +iv_g\partial_x\phi_L(x,t) + i2v_g e^{i\varphi}\phi_R(-x,t)\delta(x) \\ &\quad + V\delta(x+d)e_2(t)e^{-i\omega_{12}t}, \qquad (10b) \\ i\partial_t e_2(t) &= V[\phi_R(-d,t)+\phi_L(-d,t)]e^{i\omega_{12}t}, \qquad (10c) \end{aligned}$$

where $\omega_{12} = \omega_2 - \omega_1$ is the frequency separation between the atomic states $|1\rangle$ and $|2\rangle$. The full system dynamics can be obtained by solving these equations of motion. For an arbitrary set of initial conditions, the system evolves in time according to the equations of motion to trace out the full spatiotemporal dynamics of the process. In general, the set of equations must be solved numerically. For this purpose, we have developed an efficient pseudospectral method operating on a nonuniform grid [36].

The spontaneous emission process is described by specifying $e_2(t=0) = 1$ and all other initial amplitudes equal to zero, i.e., the atom is initially excited and no photon is present. Numerical results will be presented in Sec. III C 1. For spontaneous emission, it turns out that the photonic degree of freedom can be completely eliminated, yielding a single intuitive first-order delay-differential equation for the atomic excitation amplitude

$$\dot{e}_2(t) + g_0 e_2(t) + g_0\theta(t-2T)e_2(t-2T)e^{i2\omega_{12}T+i\varphi} = 0. \qquad (11)$$

Here, $\theta(\cdot)$ is a Heaviside step function, $g_0 = V^2/v_g$ is the decay rate for the no-boundary case, and $T \equiv d/v_g$ is the propagation time between the atom and the boundary in the waveguide with group velocity v_g and d the spatial separation between the boundary and the atom. Compared to the no-boundary case [Eq. (1)], there is an additional term representing the delayed, phase-shifted feedback introduced by the boundary. The delay amount $2T$ is the round-trip propagation time in between the atom and the boundary. Similarly, the phase consists of the round-trip propagation phase $2\omega_{12}T$ and the boundary induced reflection phase φ. Compared with the set of Equations (10), which necessitates a two-dimensional computation in space and time, Eq. (11) requires only a one-dimensional computation and can easily be computed with an order of magnitude efficiency improvement. To get information on the photonic modes, however, one must solve the full set of Equations (10) or use the explicit spectral representation provided in the Appendix. A detailed derivation of Eq. (11) is presented in the Appendix.

2. *Cavity QED*

In cavity QED geometry [Fig. 2(c)], the total Hamiltonian is

$$H = H_w + H_a + H_c + H_{wc} + H_{ac} + H_b. \qquad (12)$$

The waveguide, atom, and boundary terms H_w, H_a, and H_b are identical to those given in Sec. III B1. H_c is the Hamiltonian for cavity modes, and is given by

$$H_c = \hbar\omega_c a_c^\dagger a_c, \qquad (13)$$

where $a_c^\dagger$ and a_c are creation and annihilation operators for cavity modes, and ω_c is the resonant frequency of the cavity.

H_{wc} describes the coupling between guided photonic modes in the waveguide and cavity modes, and is given by

$$\begin{aligned} H_{wc} = \hbar\int_{-\infty}^{0} dx\,\delta(x+d)V_c\big\{&c_R^\dagger(x)a_c + c_L^\dagger(x)a_c \\ &+ a_c^\dagger c_R(x) + a_c^\dagger c_L(x)\big\}, \end{aligned} \qquad (14)$$

where V_c gives the coupling strength between waveguided and cavity modes.

H_{ac} describes the coupling between the atom and cavity modes, and is given by

$$H_{ac} = \hbar g(a_2^\dagger a_1 a_c + a_c^\dagger a_1^\dagger a_2), \qquad (15)$$

where g is the atom-cavity coupling strength.

The general one-photon state is

$$\begin{aligned} |\psi\rangle = &\int_{-\infty}^{0} dx\,\phi_R(x,t)e^{-i\omega_1 t}c_R^\dagger(x)a_1^\dagger|0\rangle \\ &+ \int_{-\infty}^{0} dx\,\phi_L(x,t)e^{-i\omega_1 t}c_L^\dagger(x)a_1^\dagger|0\rangle \\ &+ e_c(t)e^{-i(\omega_c+\omega_1)t}a_c^\dagger a_1^\dagger|0\rangle + e_2(t)e^{-i\omega_2 t}a_2^\dagger|0\rangle, \end{aligned} \qquad (16)$$

where $\phi_R(x,t)$ and $\phi_L(x,t)$ are again amplitudes of right- and left-moving photonic modes in the waveguide, $e_c(t)$ is the cavity mode excitation amplitude, and $e_2(t)$ is the excitation amplitude of the atom. In Eq. (16), the phase due to the temporal evolution of the atomic and cavity states is written explicitly for convenience.

Solving Schrödinger's equation with the given Hamiltonian and state yields the equations of motion

$$\begin{aligned} i\partial_t\phi_R(x,t) &= -iv_g\partial_x\phi_R(x,t) - i2v_g e^{-i\varphi}\phi_L(-x,t)\delta(x) \\ &\quad + V_c\delta(x+d)e_c(t)e^{-i\omega_c t}, \qquad (17a) \\ i\partial_t\phi_L(x,t) &= +iv_g\partial_x\phi_L(x,t) + i2v_g e^{i\varphi}\phi_R(-x,t)\delta(x) \\ &\quad + V_c\delta(x+d)e_c(t)e^{-i\omega_c t}, \qquad (17b) \\ i\partial_t e_c(t) &= V_c[\phi_R(-d,t)+\phi_L(-d,t)]e^{i\omega_c t} + ge_2(t)e^{i\Delta t}, \\ i\partial_t e_2(t) &= ge_c(t)e^{-i\Delta t}, \qquad (17d) \end{aligned}$$

where $\Delta \equiv \omega_c - \omega_{12}$ gives the frequency detuning of the atom and the cavity. The equations of motion (17) are general, and describe all one-photon processes. Spontaneous emission is described by setting $e_2(t=0) = 1$ and all other initial amplitudes equal to zero, and the state evolves in time according to Eqs. (17).

Similarly, in this case, the photonic and cavity degrees of freedom can again be eliminated to produce an intuitive second-order delay-differential equation for the atomic excitation amplitude

$$\begin{aligned} &\ddot{e}_2(t) + (\Gamma + i\Delta)\dot{e}_2(t) + \Gamma\theta(t-2T)\dot{e}_2(t-2T)e^{i2\omega_{12}T+i\varphi} \\ &\quad + g^2 e_2(t) = 0, \end{aligned} \qquad (18)$$

which can be computed efficiently. Here, $\Gamma = V_c^2/v_g$ is the decay rate of the cavity in the free case. The additional term is again delayed by an amount $2T$ and has an accumulated phase due to the round-trip propagation ($2\omega_{12}T$) and reflection by the boundary (φ). A detailed derivation of Eq. (18) is provided in the Appendix.

C. Numerical results and discussion

In this section, we discuss the effects of a boundary on the temporal behavior of the atomic excitation and the corresponding effects on the emitted photonic wave packet. Due to the feedback provided by a boundary, the large-time excitation can be either reduced or significantly increased, depending on the nature of the interference. The temporal response of the atomic excitation in such a situation cannot be described by a single characteristic time scale. Hereafter, we use "lifetime" to refer to the value of the atomic excitation in the large-time limit. The emitted photonic wave packet is correspondingly modified, and the emitted photons can be temporally very narrow or very broad. We also discuss the effect of atomic dissipation, which can weaken the effect of a boundary on the spontaneous emission process.

1. Atomic excitation

The temporal behavior of the atomic excitation in waveguide QED geometry is shown in Fig. 4, which was generated by solving Eq. (11) with $e_2(0) = 1$. As dictated by causality, the excitation follows exponential decay as for a bi-infinite waveguide [Eq. (1)] for $t < 2T$. For $t > 2T$, reflected modes have had a chance to return to the atom, where they interfere with the emitted modes as described previously. Destructive interference ($2\omega_{12}T + \varphi = 2\pi\,[n + 1/2]$) inhibits

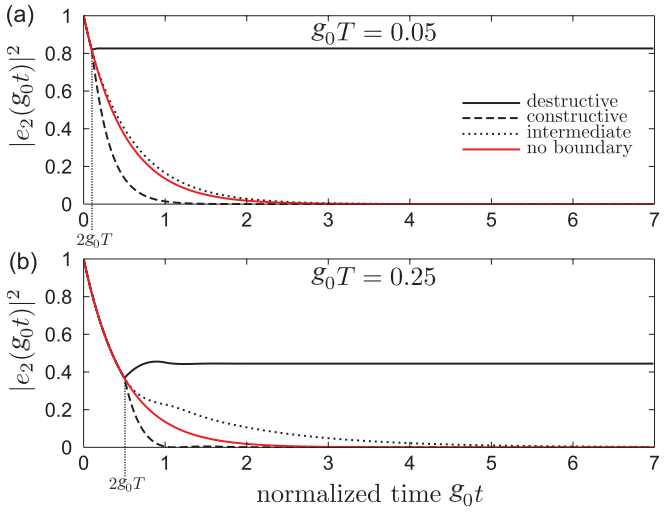

FIG. 4. (Color online) Atomic excitation for the waveguide QED case as in Fig. 2(a), showing effects of destructive [$2\omega_{12}T + \varphi = (2n + 1)\pi$], constructive ($2\omega_{12}T + \varphi = 2n\pi$), and intermediate [$2\omega_{12}T + \varphi = (2n + 1/2)\pi$] interference between reflected and emitted photonic modes. (a) $g_0T = 0.05$. (b) $g_0T = 0.25$. In each figure, ω_{12} is chosen such that $2\omega_{12}T = (2n + 1)\pi$ and φ is varied. Alternatively, the same figure can be obtained by fixing φ and varying ω_{12}.

emission into guided modes, giving rise to very long-lived atomic excitation. Compared to the no-boundary case, such destructive interference can lead to an excitation lifetime that is practically only limited by dissipation. For example, for $g_0T = 0.05$ [Fig. 4(a)], destructive interference gives rise to an atomic excitation probability $|e_2(g_0t)|^2$ that is more than an order of magnitude greater than the no-boundary response at $g_0t = 1.5$. On the other hand, constructive interference ($2\omega_{12}T + \varphi = 2\pi n$) enhances the rate of decay into guided modes, so the atom relaxes to its ground state more quickly.

Figure 5 shows the temporal behavior of the atomic excitation in cavity QED geometry, which was computed by solving Eq. (18) with $e_2(0) = 1$ and $\dot{e}_2(0) = 0$, where the second initial condition is equivalent to no initial cavity excitation [i.e., $e_c(0) = 0$] by Eq. (17d). Again, the atomic excitation must follow the no-boundary harmonic oscillator solutions given by Eq. (2) for $t < 2T$. While the excitation does depart from the no-boundary solution for $t > 2T$, the departure is generally smoother than for the waveguide QED case (i.e., there will not be a cusp at $t = 2T$), due to the buffering effect of the cavity. Mathematically, this is a direct consequence of the order of the governing differential equation in each case. The interference due to the relative phase $2\omega_{12}T + \varphi$ again determines the nature of the deviation. The atomic response just after $t = 2T$, however, is very different from that in the waveguide QED case: Destructive interference causes a short-term (i.e., just after $t = 2T$) enhancement of atomic decay, while constructive interference causes a short-term suppression of the atomic decay. Due to the additional dynamics introduced by the cavity, the long-term ($t \gg 2T$) effect on the temporal behavior cannot be described simply by an enhanced or suppressed decay rate. Rather, constructive interference causes the excitation to appear more overdamped (less oscillatory, with slower decay as the effective damping increases), while destructive interference drives the system toward underdamped (more oscillatory).

Cavity-atom frequency detuning Δ also suppresses atomic decay, as the cavity cannot efficiently support the modes emitted by the atom. For a given atom-cavity coupling strength g, detuning has a stronger influence when the effective damping is small (i.e., Γ is small or the system exhibits destructive interference).

2. Emitted photonic modes

As the presence of a boundary changes the temporal response of the atom, the emitted photonic wave packet is correspondingly modified. Figure 6(a) shows the emitted photonic wave forms for the waveguide QED case. With no boundary, the emitted photons will always have an exponential envelope [Fig. 6(a1)], corresponding to the exponential decay of the atomic excitation. When a boundary is introduced, the emitted pulse, which has the form $\phi_L(t + x/v_g)$, follows the exponentially decaying no-boundary profile for $0 < t + x/v_g < 2T$. For $t + x/v_g > 2T$, the amplitude is much higher for constructive interference or near zero for destructive interference. For constructive interference [Figs. 6(a), 2 and 6(a), 5], the enhanced emission for $t > 2T$ will produce a second photonic peak at $t + x/v_g = 2T$. For

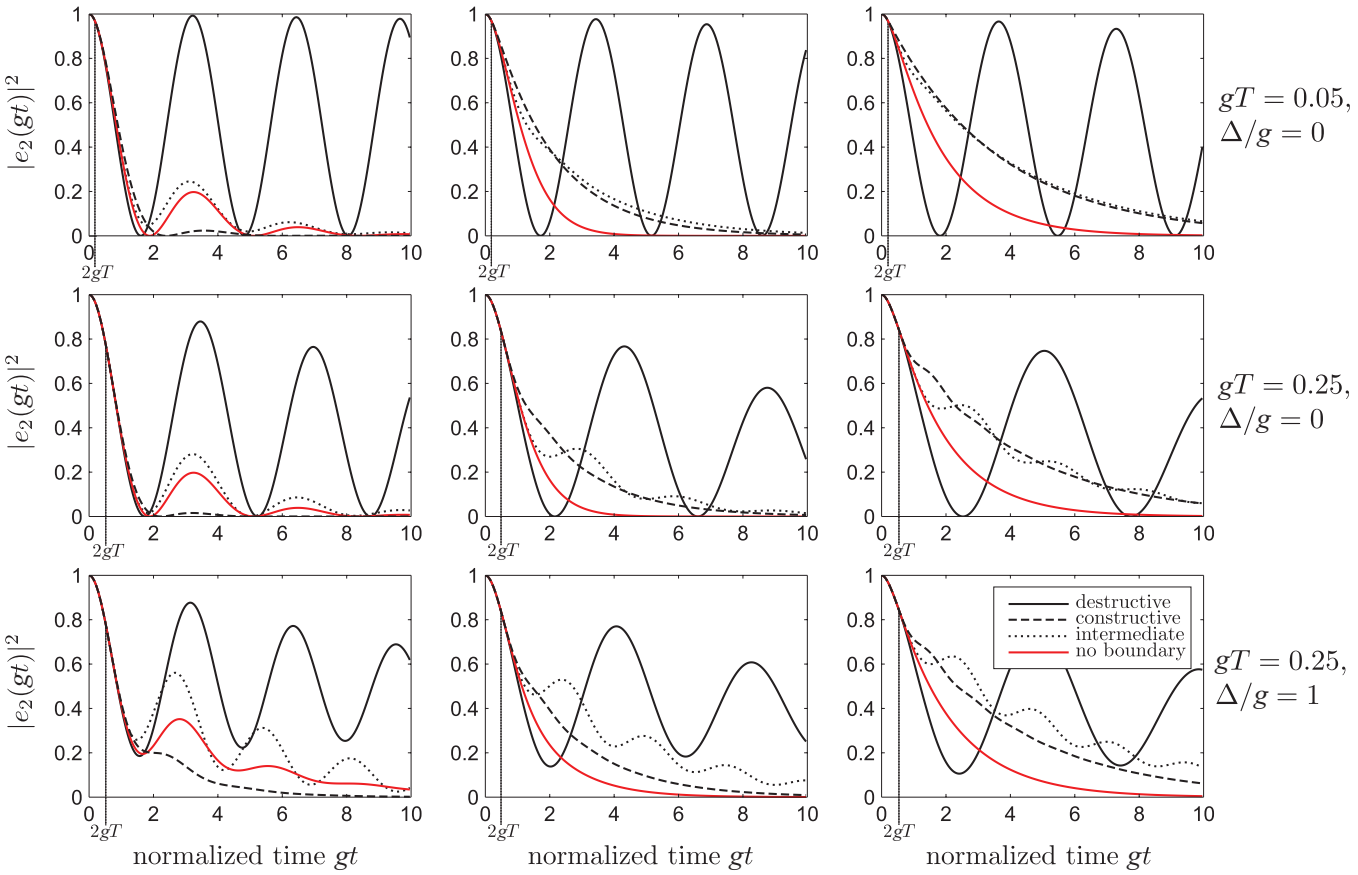

FIG. 5. (Color online) Atomic excitation for the cavity QED case [Fig. 2(c)], showing effects of interference, cavity-waveguide coupling strength, and cavity-atom detuning. Left column: underdamped ($\Gamma/g = 0.5$). Center column: critically damped ($\Gamma/g = 2$). Right column: overdamped ($\Gamma/g = 3.5$).

destructive interference [Figs. 6(a), 4 and 6(a), 7], the temporal width of the photon can be strongly suppressed.

Figure 6(b) shows the emitted photonic profiles for the cavity QED case. Without a boundary, the general behavior corresponds to the atomic excitation behavior with a cavity: An underdamped system leads to oscillatory photonic profiles, while an overdamped system leads to photonic profiles which resemble a smoothed exponential decay [Fig. 6(b), 1]. When a boundary is present, constructive interference [Figs. 6(b), 2 and 6(b), 5] causes them to look more overdamped (nonoscillatory), while destructive interference [Figs. 6(b), 4 and 6(b), 7] generally causes the emitted photons to look more underdamped (oscillatory).

3. *Dissipation*

When atomic dissipation γ_0 is included in the waveguide QED case [Fig. 2(a)], Eq. (11) becomes

$$\dot{e}_2(t) + (g_0 + \gamma_0)e_2(t) + g_0\theta(t - 2T)e_2(t - 2T)e^{i2\omega_{12}T + i\varphi} = 0, \tag{19}$$

where γ_0 is added to g_0 in the nonfeedback term. Figure 7 shows the atomic excitation in the presence of dissipation. There is still a period of free exponential decay for $t < 2T$, though the decay rate is now $g_0 + \gamma_0$. For $t > 2T$, constructive interference still leads to faster decay, while destructive interference still retards decay. In each case, however, the effect is degraded by the presence of dissipation. For small dissipation [Fig. 7(b)], the feedback from the boundary can still keep the atom excited for much longer than the no-boundary case. As dissipation further increases [Figs. 7(c) and 7(d)], all effects from the boundary are dominated by dissipation.

When dissipation is included in the cavity QED case [Fig. 2(c)], Eq. (18) becomes

$$\begin{aligned}&\ddot{e}_2(t) + (\Gamma + i\Delta + \gamma_c + \gamma)\dot{e}_2(t) \\ &\quad + \Gamma\theta(t - 2T)\dot{e}_2(t - 2T)e^{i2\omega_{12}T + i\varphi} \\ &\quad + [g^2 + \gamma(\Gamma + i\Delta + \gamma_c)]e_2(t) \\ &\quad + \gamma\Gamma\theta(t - 2T)e_2(t - 2T)e^{i2\omega_{12}T + i\varphi} = 0,\end{aligned} \tag{20}$$

where γ and γ_c are the atomic and cavity dissipation parameters, respectively. Figure 8 shows atomic excitation with a cavity in the presence of dissipation. From the point of view of the atom, cavity dissipation and cavity leakage into the waveguide appear as the same mechanism except that modes escaping through dissipation do not contribute to feedback from the boundary. As shown in Fig. 8, increasing γ_c makes the excitation appear more overdamped and reduces the effect of boundary-induced interference. When $\gamma_c > \Gamma$, the effects of interference become almost negligible. Atomic dissipation γ, on the other hand, has the same effect as coupling to free space. That is, increasing γ causes the excitation

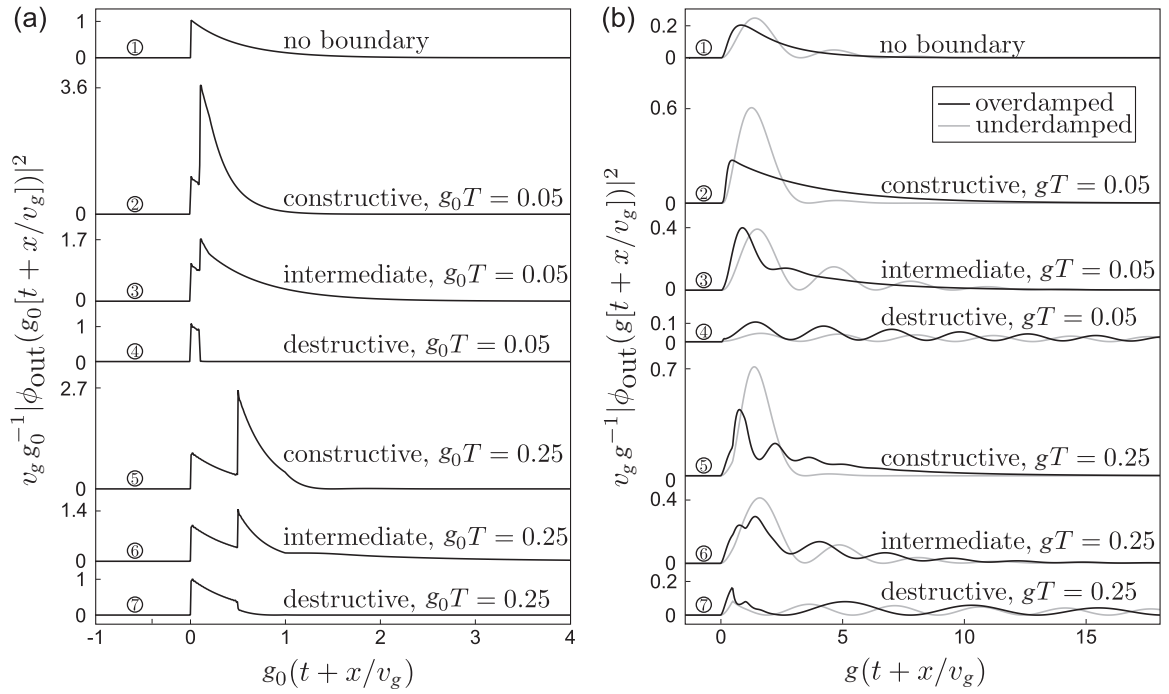

FIG. 6. Output photonic modes with a boundary. (a) Waveguide QED. (b) Cavity QED, for both $\Gamma/g = 3.5$ (overdamped) and $\Gamma/g = 0.5$ (underdamped).

to resemble exponential decay, regardless of the cavity and boundary parameters.

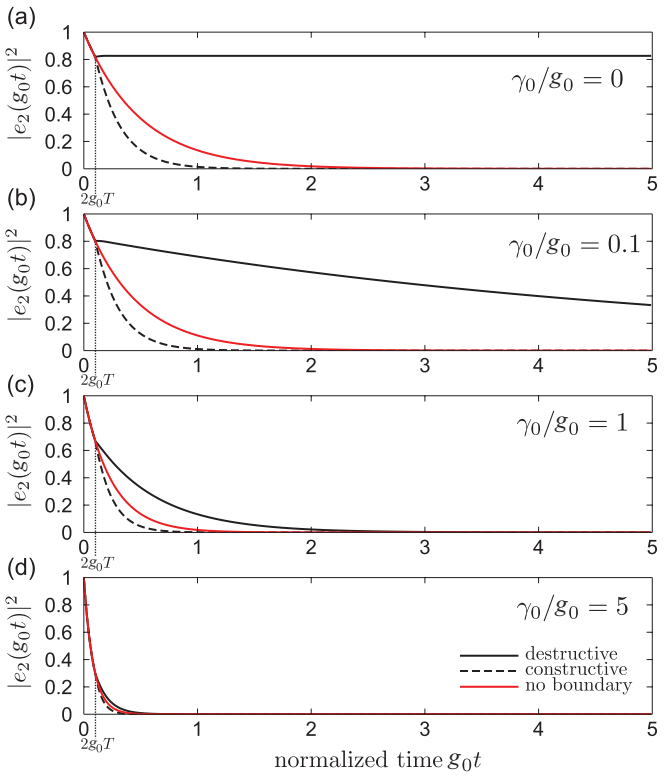

FIG. 7. (Color online) Atomic excitation for the waveguide QED case [Fig. 2(a)], showing effects dissipation. (a) $\gamma_0/g_0 = 0$. (b) $\gamma_0/g_0 = 0.1$. (c) $\gamma_0/g_0 = 1$. (d) $\gamma_0/g_0 = 5$. $g_0T = 0.05$ for all plots.

Here we show that temporally delayed interference is effective in controlling atomic decay by providing a realistic estimate using parameters from some state-of-the-art experiments. In waveguide QED, it has been demonstrated that the atom can emit photons preferentially into the waveguide. Values of γ_0/g_0 as low as 0.18 over a large bandwidth of 10 THz have been theoretically predicted for a quantum dot coupled to a photonic crystal waveguide [8], and even lower values of $\gamma_0/g_0 = 0.12$ have been experimentally measured, albeit over a smaller bandwidth [7]. These ratios are close to those in Fig. 7(b), indicating that the atom can be controlled effectively under current experimental conditions. In cavity QED, strong coupling of an atom to a cavity has been experimentally demonstrated. Moreover, to efficiently control spontaneous emission when a waveguide is coupled to the cavity, optimal coupling between the cavity and the waveguide is also crucial. In Ref. [37], strong coupling between the quantum dot and the cavity has been shown ($g/2\pi = 21$ GHz and $\gamma/2\pi = 6.3$ GHz) but the cavity is undercoupled to the waveguide ($\Gamma/2\pi = 3.4$ GHz and $\gamma_c/2\pi = 52.6$ GHz). Reference [38] demonstrates that the waveguide-cavity coupling can be greatly improved (i.e., lower γ_c, with $\Gamma/2\pi = 5.2$ GHz and $\gamma_c/2\pi = 4.2$ GHz), leading to a situation close to the one in Fig. 8 with $\gamma/g = 0.1$, $\gamma_c/g = 0.1$, and $\Gamma/g = 0.5$. Therefore, within current experimental reach, our scheme based on delayed feedback interference is effective to control the decay of atomic excitation and achieve a much longer photon storage time in both waveguide QED and cavity QED.

IV. CONCLUSION

In this paper we have presented the theory of single-photon scattering by a two-level atom in the presence of

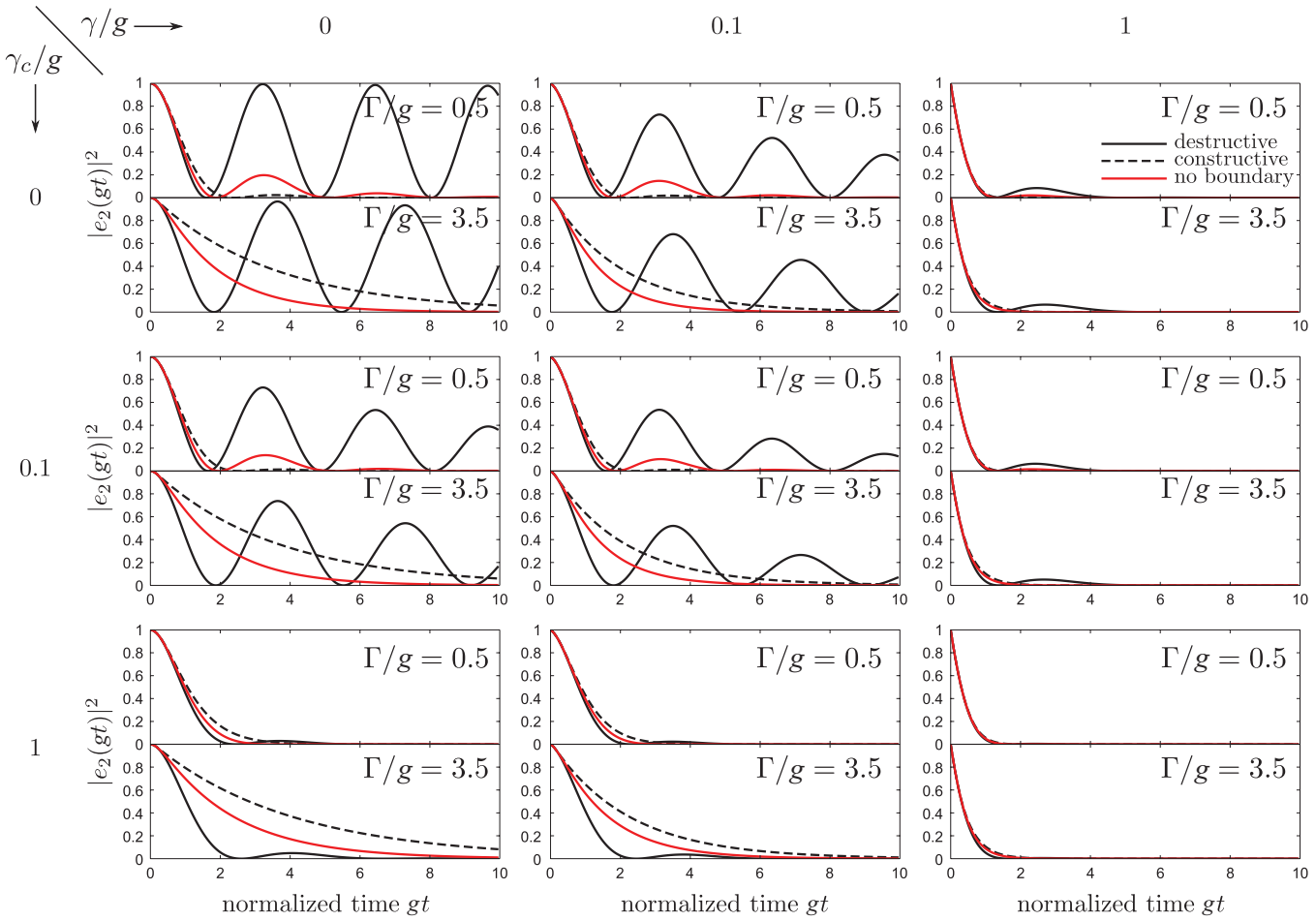

FIG. 8. (Color online) Atomic excitation in cavity QED [Fig. 2(c)], showing effects of dissipation. For all plots, $gT = 0.05$ and $\Delta = 0$.

a nanophotonic boundary in cavity QED. In particular, we applied this theoretical machinery to one of the most fundamental nanophotonic processes, spontaneous emission, and showed that a boundary can radically modify the temporal behavior of the process and change the time scale of the process by orders of magnitude. The theoretical framework, however, describes all such single-photon processes and can equally be used to investigate, for example, efficient photon capture using a two-level atom near a boundary. Furthermore, additional control of spontaneous emission could be achieved by modulating the boundary to control the reflection phase. By slowly modulating the boundary, one could switch between inhibition and acceleration of spontaneous emission without significantly perturbing the short-term behavior of the process. On the other hand, by quickly modulating the reflection phase, one could introduce new frequency components to the reflected photon, providing a higher degree of control over the interference. It remains as an interesting question whether arbitrary single-photon wave forms can be engineered by properly modulating the boundary. Finally, the theory presented here can be readily extended to describe multiphoton scattering in cavity QED. The ability to handle multiple-photon processes would allow us to investigate the effects of a boundary on other fundamental processes such as stimulated emission, or to design active control schemes, whereby the emission from an excited atom is delayed or triggered by an input photon. Spatially extended entanglement of photon pairs could also be created with a two-level atom near a boundary due to the prolonged atom-photon interaction time afforded by a boundary.

APPENDIX

1. Atomic Hamiltonian using Pauli spin operators

Here we present the atomic Hamiltonian given by Eq. (6) in the main text in terms of Pauli spin operators. The equivalent Hamiltonian is

$$H_a = \hbar\left(\omega_a \mathbb{1} + \tfrac{1}{2}\omega_{12}\sigma_z\right), \tag{A1}$$

where $\omega_a = (\omega_1 + \omega_2)/2$, $\mathbb{1}$ is the identity operator, and $\omega_{12} = \omega_2 - \omega_1$ is the atomic transition frequency. The operator σ_z is

$$\sigma_z = a_2^\dagger a_2 - a_1^\dagger a_1, \tag{A2}$$

so σ_z acts on the atomic ground and excited states ($|1\rangle$ and $|2\rangle$, respectively) with $\sigma_z|1\rangle = -|1\rangle$ and $\sigma_z|2\rangle = +|2\rangle$. We note that the two equivalent atomic Hamiltonians yield identical results when acting on the atomic states.

2. Boundary Hamiltonian

Here we develop the boundary Hamiltonian given in Eq. (8). We begin by considering the free Hamiltonian for a bi-infinite

waveguide with no atom, analogous to that given by Eq. (5),

$$H_{\text{free}} = \int_{-\infty}^{\infty} dx\, \hbar\{c_R^\dagger(x)(-iv_g\partial_x)c_R(x) + c_L^\dagger(x)(+iv_g\partial_x)c_L(x)\}, \tag{A3}$$

so

$$|\psi\rangle_{\text{free}} = e^{ikx}c_R^\dagger(x)|0\rangle + e^{-ikx}c_L^\dagger(x)|0\rangle \tag{A4}$$

is an eigenstate of the free Hamiltonian, satisfying

$$H_{\text{free}}|\psi\rangle_{\text{free}} = \hbar v_g k|\psi\rangle_{\text{free}}. \tag{A5}$$

With a boundary, the state

$$|\psi\rangle = \theta(-x)e^{ikx}c_R^\dagger(x)|0\rangle + \theta(-x)e^{-ikx+i\varphi}c_L^\dagger(x)|0\rangle \tag{A6}$$

will be an eigenstate of the total Hamiltonian, which will be a sum of free and boundary terms

$$H = H_{\text{free}} + H_b, \tag{A7}$$

satisfying

$$H|\psi\rangle = \hbar v_g k|\psi\rangle, \tag{A8}$$

so

$$H_b|\psi\rangle = (\hbar v_g k - H_{\text{free}})|\psi\rangle. \tag{A9}$$

The action of the free Hamiltonian on the bounded eigenstate is

$$\begin{aligned} H_{\text{free}}|\psi\rangle &= \left(\int_{-\infty}^{\infty} dx'\,\hbar\{c_R^\dagger(x')(-iv_g\partial_{x'})c_R(x') + c_L^\dagger(x')(+iv_g\partial_{x'})c_L(x')\}\right)(\theta(-x)e^{ikx}c_R^\dagger(x)|0\rangle \\ &\quad + \theta(-x)e^{-ikx+i\varphi}c_L^\dagger(x)|0\rangle), \qquad \text{(A10)} \\ &= -i\hbar v_g\partial_x[\theta(-x)e^{ikx}]c_R^\dagger(x)|0\rangle + i\hbar v_g\partial_x[\theta(-x) \\ &\quad \times e^{-ikx+i\varphi}]c_L^\dagger(x)|0\rangle, \qquad \text{(A11)} \\ &= \hbar v_g k[\theta(-x)e^{ikx}c_R^\dagger(x)|0\rangle + \theta(-x)e^{-ikx+i\varphi} \\ &\quad \times c_L^\dagger(x)|0\rangle] + i\hbar v_g\delta(x)e^{ikx}c_R^\dagger(x)|0\rangle \\ &\quad - i\hbar v_g\delta(x)e^{-ikx+i\varphi}c_L^\dagger(x)|0\rangle, \qquad \text{(A12)} \\ &= \hbar v_g k|\psi\rangle + i\hbar v_g\delta(x)e^{ikx}c_R^\dagger(x)|0\rangle - i\hbar v_g\delta(x) \\ &\quad \times e^{-ikx+i\varphi}c_L^\dagger(x)|0\rangle, \qquad \text{(A13)} \end{aligned}$$

so

$$\begin{aligned} H_b|\psi\rangle &= \hbar v_g k|\psi\rangle - H_{\text{free}}|\psi\rangle, \qquad \text{(A14)} \\ &= -i\hbar v_g\delta(x)e^{ikx}c_R^\dagger(x)|0\rangle \\ &\quad + i\hbar v_g\delta(x)e^{-ikx+i\varphi}c_L^\dagger(x)|0\rangle. \qquad \text{(A15)} \end{aligned}$$

Now, we check the action of the proposed form of H_b [Eq. (8)] on the bounded eigenstate

$$\begin{aligned} H_b|\psi\rangle &= \hbar\int_{-\infty}^{0^+} dx'\,\delta(x')[i2v_g e^{i\varphi}c_L^\dagger(-x')c_R(x') \\ &\quad - i2v_g e^{-i\varphi}c_R^\dagger(-x')c_L(x')][\theta(-x)e^{ikx}c_R^\dagger(x)|0\rangle \\ &\quad + \theta(-x)e^{-ikx+i\varphi}c_L^\dagger(x)|0\rangle], \qquad \text{(A16)} \\ &= \hbar\int_{-\infty}^{0^+} dx'\,\delta(x')[i2v_g e^{i\varphi}c_L^\dagger(-x')c_R(x')]\theta(-x)e^{ikx}c_R^\dagger(x)|0\rangle \\ &\quad + \hbar\int_{-\infty}^{0^+} dx'\,\delta(x')[-i2v_g e^{-i\varphi}c_R^\dagger(-x')c_L(x')]\theta(-x) \\ &\quad \times e^{-ikx+i\varphi}c_L^\dagger(x)|0\rangle, \qquad \text{(A17)} \\ &= -i\hbar 2v_g\delta(x)\theta(x)e^{ikx}c_R^\dagger(x)|0\rangle + i\hbar 2v_g\delta(x)\theta(x) \\ &\quad \times e^{-ikx+i\varphi}c_L^\dagger(x)|0\rangle, \qquad \text{(A18)} \end{aligned}$$

so with $\delta(x)\theta(x) \to \frac{1}{2}\delta(x)$, one has

$$H_b|\psi\rangle = -i\hbar v_g\delta(x)e^{ikx}c_R^\dagger(x)|0\rangle + i\hbar v_g\delta(x)e^{-ikx+i\varphi}c_L^\dagger(x)|0\rangle, \tag{A19}$$

so the proposed boundary Hamiltonian given by Eq. (8) satisfies the condition given in Eq. (A15).

3. Derivation of delay-differential equations for atomic response

In this section, we derive Eqs. (11) and (18) for the atomic excitation in the waveguide QED [Fig. 2(a)] and cavity QED [Fig. 2(c)] cases, respectively. Equations (11) and (18) describe the temporal behavior in a manner that can be computed very efficiently when compared with the full equations of motion (10) or (17).

a. Waveguide QED

Here we derive Eq. (11) for the atomic excitation in the waveguide QED case. When there are no initial photonic modes and the atom is initially excited, right-moving modes will exist only in the region $-d < x < 0$, while left-moving modes will exist in two distinct functional forms in the regions $x < -d$ and $-d < x < 0$. Since the waveguide is nondispersive, the functions describing the photonic modes in each region will be functions only of $t - x/v_g$ (for right-moving modes) or $t + x/v_g$ (for left-moving modes). So, the photonic amplitudes $\phi_R(x,t)$ and $\phi_L(x,t)$ can be written

$$\phi_R(x,t) = [\theta(x+d) - \theta(x)]f_R(t - x/v_g), \tag{A20}$$

$$\phi_L(x,t) = [\theta(x+d) - \theta(x)]f_L(t + x/v_g) + \theta[-(x+d)]g_L(t + x/v_g), \tag{A21}$$

where $\theta(\cdot)$ is a step function and $f_R(t - x/v_g)$, $f_L(t + x/v_g)$, and $g_L(t + x/v_g)$ describe photonic modes moving to the right $(-)$ or left $(+)$ in each region.

Using the forms given by Eqs. (A20) and (A21) in Eq. (10a), one has

$$\begin{aligned} &i[\theta(x+d) - \theta(x)]\frac{\partial}{\partial t}f_R(t - x/v_g) \\ &\quad = -iv_g[\delta(x+d) - \delta(x)]f_R(t - x/v_g) \\ &\quad\quad - iv_g[\theta(x+d) - \theta(x)]\frac{\partial}{\partial x}f_R(t - x/v_g) \\ &\quad\quad - i2v_g e^{-i\varphi}\delta(x)\{[\theta(x+d) - \theta(x)]f_L(t + x/v_g) \\ &\quad\quad + \theta[-(x+d)]g_L(t + x/v_g)\} + V\delta(x+d)e_2(t)e^{-i\omega_{12}t}, \end{aligned} \tag{A22}$$

but by the chain rule, $\frac{\partial}{\partial t} = \frac{\partial}{\partial(t-x/v_g)}$ and $\frac{\partial}{\partial x} = -\frac{1}{v_g}\frac{\partial}{\partial(t-x/v_g)}$, so the left-hand side of Eq. (A22) cancels the second term on the right-hand side, yielding

$$\begin{aligned} & iv_g[\delta(x+d)-\delta(x)]f_R(t-x/v_g) \\ & \quad = -i2v_g e^{-i\varphi}\delta(x)\{[\theta(x+d)-\theta(x)]f_L(t+x/v_g) \\ & \qquad + \theta[-(x+d)]g_L(t+x/v_g)\} + V\delta(x+d)e_2(t)e^{-i\omega_{12}t}. \end{aligned} \tag{A23}$$

Now, considering terms proportional to $\delta(x+d)$ in Eq. (A23), one obtains

$$f_R(t+d/v_g) = -\frac{iV}{v_g}e_2(t)e^{-i\omega_{12}t}, \tag{A24}$$

so

$$f_R(t) = -\frac{iV}{v_g}e_2(t-d/v_g)e^{-i\omega_{12}(t-d/v_g)}, \tag{A25}$$

and considering terms proportional to $\delta(x)$ in Eq. (A23), one obtains

$$f_R(t) = e^{-i\varphi}f_L(t), \tag{A26}$$

so

$$f_L(t) = -\frac{iV}{v_g}e_2(t-d/v_g)e^{-i\omega_{12}(t-d/v_g)+i\varphi} \tag{A27}$$

or

$$f_L(t-d/v_g) = -\frac{iV}{v_g}e_2(t-2d/v_g)e^{-i\omega_{12}(t-2d/v_g)+i\varphi}. \tag{A28}$$

Now, using the forms given by Eqs. (A20) and (A21) in Eq. (10b), one obtains

$$\begin{aligned} & i[\theta(x+d)-\theta(x)]\frac{\partial}{\partial t}f_L(t+x/v_g) + i\theta[-(x+d)]\frac{\partial}{\partial t}g_L(t+x/v_g) \\ & \quad = iv_g[\delta(x+d)-\delta(x)]f_L(t+x/v_g) + iv_g[\theta(x+d)-\theta(x)]\frac{\partial}{\partial x}f_L(t+x/v_g) - iv_g\delta(x+d)g_L(t+x/v_g) \\ & \qquad + iv_g\theta[-(x+d)]\frac{\partial}{\partial x}g_L(t+x/v_g) + i2v_g e^{i\varphi}[\theta(x+d)-\theta(x)]f_R(t-x/v_g) + V\delta(x+d)e_2(t)e^{-i\omega_{12}t}. \end{aligned} \tag{A29}$$

Again, using the chain rule, the left-hand side of Eq. (A29) cancels with the right-hand side terms proportional to $\partial/\partial x$, yielding

$$\begin{aligned} & -iv_g[\delta(x+d)-\delta(x)]f_L(t+x/v_g) + iv_g\delta(x+d)g_L(t+x/v_g) \\ & \quad = i2v_g e^{i\varphi}[\theta(x+d)-\theta(x)]f_R(t-x/v_g) + V\delta(x+d)e_2(t)e^{-i\omega_{12}t}. \end{aligned} \tag{A30}$$

Considering terms proportional to $\delta(x)$ in Eq. (A30) will only recover Eq. (A26). Considering terms proportional to $\delta(x+d)$, one has

$$-iv_g f_L(x-d/v_g) + iv_g g_L(t-d/v_g) = Ve_2(t)e^{-i\omega_{12}t}, \tag{A31}$$

so combining Eqs. (A28) and (A31), one has

$$\begin{aligned} g_L(t-x/v_g) = & -\frac{iV}{v_g}e_2(t-2d/v_g)e^{-i\omega_{12}(t-2d/v_g)+i\varphi} \\ & -\frac{iV}{v_g}e_2(t)e^{-i\omega_{12}t}. \end{aligned} \tag{A32}$$

Finally, using the forms given by Eqs. (A20) and (A21) in Eq. (10c), one has

$$\begin{aligned} i\dot{e}_2(t) = V\{ & [\theta(0)-\theta(-d)]f_R(t+d/v_g) \\ & + [\theta(0)-\theta(-d)]f_L(t-d/v_g) \\ & + \theta(0)g_L(t-d/v_g)\}e^{i\omega_{12}t}. \end{aligned} \tag{A33}$$

So, using $\theta(0) = 1/2$ and combining Eqs. (A33), (A24), (A28), and (A32), one obtains a single first-order delay-differential equation for the atomic excitation

$$\dot{e}_2(t) + g_0 e_2(t) + g_0\theta(t-2T)e_2(t-2T)e^{i2\omega_{12}T+i\varphi} = 0, \tag{A34}$$

where $\theta(\cdot)$ comes in as a consequence of the round-trip propagation delay and $T = d/v_g$ is the propagation time between the atom and the boundary. This delay-differential equation encapsulates in a much simpler way the spontaneous emission behavior of the system when compared with the full equations of motion (10). Note that the governing equation (1) for a bi-infinite waveguide can be recovered by setting the delayed term to zero.

b. Cavity QED

For the cavity QED case, we begin by differentiating both sides of Eq. (17d) with respect to time to get

$$\ddot{e}_2(t)e^{i\Delta t} + i\Delta\dot{e}_2(t)e^{i\Delta t} = -ig\dot{e}_c(t). \tag{A35}$$

The photonic modes can again be written as

$$\phi_R(x,t) = [\theta(x+d)-\theta(x)]f_R(t-x/v_g), \tag{A36}$$

$$\begin{aligned} \phi_L(x,t) = & [\theta(x+d)-\theta(x)]f_L(t+x/v_g) \\ & + \theta[-(x+d)]g_L(t+x/v_g), \end{aligned} \tag{A37}$$

so following a procedure analogous to that given in the previous section, one obtains

$$f_R(t+d/v_g) = -\frac{iV_c}{v_g}e_c(t)e^{-i\omega_c t}, \tag{A38}$$

$$f_L(t-d/v_g) = -\frac{iV_c}{v_g}e_c(t-2d/v_g)e^{-i\omega_c(t-2d/v_g)+i\varphi}, \quad \text{(A39)}$$

$$g_L(t-d/v_g) = -\frac{iV_c}{v_g}e_c(t-2d/v_g)e^{-i\omega_c(t-2d/v_g)+i\varphi} - \frac{iV_c}{v_g}e_c(t)e^{-i\omega_c t}, \quad \text{(A40)}$$

and using the forms given by Eqs. (A36) and (A37) in Eq. (17c), one has

$$i\dot{e}_2(t) = V_c\{[\theta(0)-\theta(-d)]f_R(t+d/v_g) + [\theta(0)-\theta(-d)]f_L(t-d/v_g) + \theta(0)g_L(t-d/v_g)\}e^{i\omega_c t} + ge_2(t)e^{i\Delta t}. \quad \text{(A41)}$$

So, using $\theta(0) = 1/2$ and combining Eqs. (A38), (A39), (A40), and (A41), one has

$$i\dot{e}_c(t) = -i\Gamma e_c(t) - i\Gamma\theta(t-2T)e_c(t-2T)e^{i2\omega_c T+i\varphi} + ge_2(t)e^{i\Delta t}, \quad \text{(A42)}$$

where $\Gamma = V_c^2/v_g$. Now, rearranging Eq. (17d) yields

$$e_c(t) = \frac{i}{g}\dot{e}_2(t)e^{i\Delta t}. \quad \text{(A43)}$$

Combining Eqs. (A42) and (A43), one has

$$\dot{e}_c(t) = -\frac{i\Gamma}{g}\dot{e}_2(t)e^{i\Delta t} - \frac{i\Gamma}{g}\theta(t-2T)\dot{e}_2(t-2T)e^{i\Delta t+i2\omega_{12}T+i\varphi} - ige_2(t)e^{i\Delta t}. \quad \text{(A44)}$$

Finally, combining Eqs. (A35) and (A44), one obtains

$$\ddot{e}_2(t) + (\Gamma + i\Delta)\dot{e}_2(t) + \Gamma\theta(t-2T)\dot{e}_2(t-2T)e^{i2\omega_{12}T+i\varphi} + g^2e_2(t) = 0, \quad \text{(A45)}$$

where $T = d/v_g$.

c. Dissipation

Dissipation can be included in the waveguide QED case by setting $H_a \to H_a - i\hbar\gamma_0 a_2^\dagger a_2$ in Eq. (6), which leads to a term $-i\gamma_0 e_2(t)$ on the right-hand side of Eq. (10c). From there, repeating the procedure in Appendix A 3a recovers the governing delay-differential equation (19) for the waveguide QED case with a boundary

$$\dot{e}_2(t) + (g_0+\gamma_0)e_2(t) + g_0\theta(t-2T)e_2(t-2T)e^{i2\omega_{12}T+i\varphi} = 0. \quad \text{(A46)}$$

The effect of dissipation for the waveguide QED case without a boundary is then obtained by setting the delayed term to zero:

$$\dot{e}_2(t) + (g_0+\gamma_0)e_2(t) = 0. \quad \text{(A47)}$$

The total decay rate is simply a sum of the rates of decay into the waveguide g_0 and decay into nonguided modes (as well as nonradiative decay) γ_0 since they are the same mechanism from the point of view of the atom.

For the cavity QED case, dissipation is included by setting $H_a \to H_a - i\hbar\gamma a_2^\dagger a_2$ as for the waveguide QED case and $H_c \to H_c - i\hbar\gamma_c a_c^\dagger a_c$ in Eq. (13), which will introduce the terms $-i\gamma e_2(t)$ and $-i\gamma_c e_c(t)$ on the right-hand sides of Eqs. (17d) and (17c), respectively. Repeating the procedure in the previous section with the modified equations of motion produces the governing equation (20) for the cavity QED case with a boundary

$$\ddot{e}_2(t) + (\Gamma + i\Delta + \gamma_c + \gamma)\dot{e}_2(t) + \Gamma\theta(t-2T)\dot{e}_2(t-2T)e^{i2\omega_{12}T+i\varphi} + [g^2 + \gamma(\Gamma + i\Delta + \gamma_c)]e_2(t) + \gamma\Gamma\theta(t-2T)e_2(t-2T)e^{i2\omega_{12}T+i\varphi} = 0. \quad \text{(A48)}$$

The effect of dissipation for the cavity QED case without a boundary is obtained by again setting the delayed terms to zero:

$$\ddot{e}_2(t) + (\Gamma + i\Delta + \gamma_c + \gamma)\dot{e}_2(t) + [g^2 + \gamma(\Gamma + i\Delta + \gamma_c)]e_2(t) = 0. \quad \text{(A49)}$$

4. Spectral representation of atomic response

When the atom is initially excited with no photon present, the state at time $t = 0$ in either the waveguide or cavity QED case will be

$$|\psi(t=0)\rangle = a_2^\dagger|0\rangle. \quad \text{(A50)}$$

The time evolution of the state is then obtained by applying the time evolution operator $e^{-i(H/\hbar)t}$:

$$|\psi(t)\rangle = e^{-i(H/\hbar)t}|\psi(0)\rangle, \quad \text{(A51)}$$

in each case. In the following, we project the initial state onto the normalized energy eigenstates for both waveguide and cavity QED cases to evaluate the action of the time evolution operator.

a. Waveguide QED

For waveguide QED as shown in Fig. 2(a), the energy eigenstate of the system is given by

$$|\psi^+\rangle = \int_{-\infty}^{0} dx\, \phi_R^+(x,t)e^{-i\omega_1 t}c_R^\dagger(x)a_1^\dagger|0\rangle + \int_{-\infty}^{0} dx\, \phi_L^+(x,t)e^{-i\omega_1 t}c_L^\dagger(x)a_1^\dagger|0\rangle + e_2^+(t)e^{-i\omega_2 t}a_2^\dagger|0\rangle. \quad \text{(A52)}$$

For $|\psi^+\rangle$ to be an eigenstate requires the time dependencies

$$\phi_R^+(x,t) = \phi_R^+(x)e^{-i\omega t}, \quad \text{(A53)}$$

$$\phi_L^+(x,t) = \phi_L^+(x)e^{-i\omega t}, \quad \text{(A54)}$$

$$e_2^+(t) = e_2(\omega)e^{-i(\omega-\omega_{12})t}, \quad \text{(A55)}$$

so that all terms in the state oscillate with the same frequency. Here, the total energy is $\hbar(\omega+\omega_1)$, corresponding to a photon with frequency ω and the atomic ground state. Now we make the ansatz on the spatial form of the scattering states

$$\phi_R^+(x) = e^{i(\omega/v_g)x}\theta[-(x+d)] + t_1(\omega)e^{i(\omega/v_g)x}(\theta[x+d]-\theta[x]), \quad \text{(A56)}$$

$$\phi_L^+(x) = t_2(\omega)e^{-i(\omega/v_g)x+i\varphi}\theta[-(x+d)] + t_1(\omega)e^{-i(\omega/v_g)x+i\varphi}(\theta[x+d]-\theta[x]), \quad \text{(A57)}$$

where $t_1(\omega)$, $t_2(\omega)$, and $e_2(\omega)$ are transmission and excitation amplitudes. Solving the equations of motion (10) with the specified scattering states yields the transmission and excitation amplitudes

$$t_1(\omega) = \frac{(\omega-\omega_{12})}{(\omega-\omega_{12})+ig_0(1+e^{i(2\omega T+\varphi)})}, \tag{A58}$$

$$t_2(\omega) = \frac{(\omega-\omega_{12})-ig_0(1+e^{-i(2\omega T+\varphi)})}{(\omega-\omega_{12})+ig_0(1+e^{i(2\omega T+\varphi)})}, \tag{A59}$$

$$e_2(\omega) = \frac{\sqrt{v_g g_0}(1+e^{i(2\omega T+\varphi)})e^{-i\omega T}}{(\omega-\omega_{12})+ig_0(1+e^{i(2\omega T+\varphi)})}. \tag{A60}$$

The normalized eigenstate $|\hat{\psi}^+\rangle$ will then be

$$|\hat{\psi}^+\rangle = \frac{1}{\langle\psi^+|\psi^+\rangle^{1/2}}|\psi^+\rangle, \tag{A61}$$

where the quantity $\langle\psi^+|\psi^+\rangle$ is given by

$$\langle\psi^+|\psi^+\rangle = L + 2d|t_1(\omega)|^2 + |e_2(\omega)|^2, \tag{A62}$$

where the x domain has been artificially restricted to $[-L/2,0]$ for convenience while computing the normalized eigenstate. The semi-infinite waveguide will be recovered by letting $L\to\infty$ at the end of the calculation.

At the artificial boundary $x=-L/2$, the boundary condition

$$\phi_R^+(x=-L/2) = \phi_L^+(x=-L/2) \tag{A63}$$

is enforced, resulting in the condition

$$e^{-i(\omega/v_g)L/2} = t_2 e^{i(\omega/v_g)L/2+i\varphi}, \tag{A64}$$

so

$$t_2 e^{i(\omega/v_g)L+i\varphi} = 1 = e^{i2\pi n}, \tag{A65}$$

where $n\in\mathbb{Z}$. Furthermore, since $|t_2(\omega)|^2=1$, t_2 can be written as

$$t_2(\omega) = e^{i\varsigma(\omega)}, \tag{A66}$$

where $\varsigma(\omega)$ is given by

$$\varsigma(\omega) = 2\arctan\left(\frac{\hat{\omega}_{12}^2 - 2g_0\hat{\omega}\sin a - 2g_0^2\cos a - g_0^2(1+\cos 2a)}{\hat{\omega}_{12}^2 - 2g_0\hat{\omega}_{12}\sin a + 2g_0^2(1+\cos a) - 2g_0\hat{\omega}_{12} - 2g_0\hat{\omega}_{12}\cos a + 2g_0^2\sin a + g_0^2\sin 2a}\right), \tag{A67}$$

where the shorthand $\hat{\omega}_{12}\equiv(\omega-\omega_{12})$ and $a\equiv 2\omega T+\varphi$ have been used for convenience.

Now, from Eq. (A65)

$$e^{i(\omega/v_g)L+i\varphi+i\varsigma(\omega)} = e^{i2\pi n}, \tag{A68}$$

so

$$(\omega/v_g)L + \varphi + \varsigma(\omega) = 2\pi n, \tag{A69}$$

so the derivative $\frac{dn}{d\omega}$ is given by

$$\frac{dn}{d\omega} = \frac{1}{2\pi}\left(L/v_g + \frac{d\varsigma}{d\omega}\right), \tag{A70}$$

$$= \frac{1}{2\pi v_g}\left(L + 2d|t_1(\omega)|^2 + |e_2(\omega)|^2\right), \tag{A71}$$

$$= \frac{1}{2\pi v_g}\langle\psi^+|\psi^+\rangle. \tag{A72}$$

Now, this result can be used to project the initial state given in Eq. (A50) onto the normalized eigenstate

$$|\psi(0)\rangle = \left(\sum_n |\hat{\psi}_o^+\rangle\langle\hat{\psi}_o^+|\right)|\psi(0)\rangle, \tag{A73}$$

$$= \sum_n \frac{1}{\langle\psi^+|\psi^+\rangle}\langle\psi_o^+|\psi(0)\rangle|\psi_o^+\rangle, \tag{A74}$$

$$= \int dn \frac{1}{\langle\psi^+|\psi^+\rangle}\langle\psi_o^+|\psi(0)\rangle|\psi_o^+\rangle, \tag{A75}$$

$$= \frac{1}{2\pi v_g}\int dn\frac{d\omega}{dn}\langle\psi_o^+|\psi(0)\rangle|\psi_o^+\rangle, \tag{A76}$$

$$= \frac{1}{2\pi v_g}\int d\omega\langle\psi_o^+|\psi(0)\rangle|\psi_o^+\rangle, \tag{A77}$$

where $|\psi_o^+\rangle\equiv|\psi^+(t=0)\rangle$. Additionally, one has

$$\langle\psi_o^+|\psi(0)\rangle = e_2^*(\omega), \tag{A78}$$

so

$$|\psi(0)\rangle = \frac{1}{2\pi v_g}\int d\omega\, e_2^*(\omega)|\psi_o^+\rangle. \tag{A79}$$

The state will then evolve according to Eq. (A51):

$$|\psi(t)\rangle = e^{-i(H/\hbar)t}|\psi(0)\rangle, \tag{A80}$$

$$= \frac{1}{2\pi v_g}\int d\omega\, e_2^*(\omega)e^{-i(H/\hbar)t}|\psi_o^+\rangle. \tag{A81}$$

Acting on an eigenstate, $H|\psi\rangle=\hbar(\omega+\omega_1)|\psi\rangle$, so the time-dependent state becomes

$$|\psi(t)\rangle = \frac{1}{2\pi v_g}\int d\omega\, e^{-i(\omega+\omega_1)t}e_2^*(\omega)|\psi_o^+\rangle. \tag{A82}$$

Finally, the time-domain atomic excitation is

$$e_2(t) = \langle 0|a_2|\psi(t)\rangle e^{i\omega_2 t}, \tag{A83}$$

$$= \frac{1}{2\pi v_g}\int d\omega\, e^{-i(\omega-\omega_{12})t}\,|e_2(\omega)|^2, \tag{A84}$$

$$= \frac{1}{2\pi v_g}\int d\omega\, e^{-i(\omega-\omega_{12})t} \times\left|\frac{\sqrt{v_g g_0}(1+e^{i(2\omega T+\varphi)})e^{-i\omega T}}{(\omega-\omega_{12})+ig_0(1+e^{i(2\omega T+\varphi)})}\right|^2, \tag{A85}$$

$$= \frac{1}{2\pi}\int d\omega\, e^{-i(\omega-\omega_{12})t}\frac{2g_0\,[1+\cos(2\omega T+\varphi)]}{(\omega-\omega_{12})^2-2g_0(\omega-\omega_{12})\sin(2\omega T+\varphi)+2g_0^2\,[1+\cos(2\omega T+\varphi)]}. \tag{A86}$$

So the time-domain excitation when the atom is initially excited is essentially related to the ω-domain excitation amplitude through the Fourier transform, as would be expected, but it is the transform of the square amplitude of the excitation spectrum that gives the correct time-domain excitation.

b. Cavity QED

For the cavity QED case as in Fig. 2(c), the energy eigenstate of the system is given by

$$\begin{aligned}|\psi^+\rangle = &\int_{-\infty}^{0} dx\,\phi_R^+(x,t)e^{-i\omega_1 t}c_R^\dagger(x)a_1^\dagger|0\rangle\\ &+\int_{-\infty}^{0} dx\,\phi_L^+(x,t)e^{-i\omega_1 t}c_L^\dagger(x)a_1^\dagger|0\rangle\\ &+e_c^+(t)e^{-i(\omega_c+\omega_1)t}a_1^\dagger a_c^\dagger|0\rangle+e_2^+(t)e^{-i\omega_2 t}a_2^\dagger|0\rangle.\end{aligned} \tag{A87}$$

As for the waveguide QED case, $|\psi^+\rangle$ being an eigenstate requires

$$\phi_R^+(x,t)=\phi_R^+(x)e^{-i\omega t}, \tag{A88}$$

$$\phi_L^+(x,t)=\phi_L^+(x)e^{-i\omega t}, \tag{A89}$$

$$e_c^+(t)=e_c(\omega)e^{-i(\omega-\omega_c)t}, \tag{A90}$$

$$e_2^+(t)=e_2(\omega)e^{-i(\omega-\omega_{12})t}, \tag{A91}$$

where the total energy is again $\hbar(\omega+\omega_1)$. Here, $\phi_R^+(x)$ and $\phi_L^+(x)$ are again given by

$$\begin{aligned}\phi_R^+(x) = &\,e^{i(\omega/v_g)x}\theta[-(x+d)]+t_1(\omega)e^{i(\omega/v_g)x}(\theta[x+d]\\ &-\theta[x]),\end{aligned} \tag{A92}$$

$$\begin{aligned}\phi_L^+(x) = &\,t_2(\omega)e^{-i(\omega/v_g)x+i\varphi}\theta[-(x+d)]\\ &+t_1(\omega)e^{-i(\omega/v_g)x+i\varphi}(\theta[x+d]-\theta[x]),\end{aligned} \tag{A93}$$

which, when used to solve the equations of motion (17), yields

$$t_1(\omega)=\frac{(\omega-\omega_{12})(\omega-\omega_c)-g^2}{(\omega-\omega_{12})[(\omega-\omega_c)+i\Gamma(1+e^{i2\omega T+i\varphi})]-g^2}, \tag{A94}$$

$$t_2(\omega)=\frac{(\omega-\omega_{12})[(\omega-\omega_c)-i\Gamma(1+e^{-i2\omega T-i\varphi})]-g^2}{(\omega-\omega_{12})[(\omega-\omega_c)+i\Gamma(1+e^{i2\omega T+i\varphi})]-g^2}, \tag{A95}$$

$$e_c(\omega)=\frac{\sqrt{v_g\Gamma}(\omega-\omega_{12})(1+e^{i2\omega T+i\varphi})e^{-i\omega T}}{(\omega-\omega_{12})[(\omega-\omega_c)+i\Gamma(1+e^{i2\omega T+i\varphi})]-g^2}, \tag{A96}$$

$$e_2(\omega)=\frac{g\sqrt{v_g\Gamma}(1+e^{i2\omega T+i\varphi})e^{-i\omega T}}{(\omega-\omega_{12})[(\omega-\omega_c)+i\Gamma(1+e^{i2\omega T+i\varphi})]-g^2}. \tag{A97}$$

By using the same boundary conditions as in Appendix A 4a, but with the cavity QED case eigenstate and scattering and excitation amplitudes, the projection of the initial state onto the normalized eigenstates is again found to be

$$|\psi(0)\rangle=\frac{1}{2\pi v_g}\int d\omega\, e_2^*(\omega)|\psi_o^+\rangle, \tag{A98}$$

so

$$|\psi(t)\rangle=\frac{1}{2\pi v_g}\int d\omega\, e^{-i(\omega+\omega_1)t}e_2^*(\omega)|\psi_o^+\rangle. \tag{A99}$$

Finally, the time-domain atomic excitation for the cavity QED case is

$$e_2(t)=\langle 0|a_2|\psi(t)\rangle e^{i\omega_2 t}, \tag{A100}$$

$$=\frac{1}{2\pi v_g}\int d\omega\, e^{-i(\omega-\omega_{12})t}\,|e_2(\omega)|^2\,, \tag{A101}$$

$$=\frac{1}{2\pi v_g}\int d\omega\, e^{-i(\omega-\omega_{12})t}\left|\frac{g\sqrt{v_g\Gamma}(1+e^{i2\omega T+i\varphi})e^{-i(\omega T}}{(\omega-\omega_{12})[(\omega-\omega_c)+i\Gamma(1+e^{i2\omega T+i\varphi})]-g^2}\right|^2, \tag{A102}$$

$$=\frac{1}{2\pi}\int d\omega\, e^{-i(\omega-\omega_{12})t}\frac{2g^2\Gamma\,[1+\cos(2\omega T+\varphi)]}{(g^2-\hat{\omega}_{12}\hat{\omega}_c)^2+2\Gamma\hat{\omega}_{12}(g^2-\hat{\omega}_{12}\hat{\omega}_c)\sin(2\omega T+\varphi)+2\Gamma^2\hat{\omega}_{12}^2\,[1+\cos(2\omega T+\varphi)]}. \tag{A103}$$

Again, the time-domain excitation is analogous to the Fourier transform of the steady state excitation amplitude.

5. Derivation of expressions for output photonic modes

The emitted wave forms can be found by projecting onto the normalized energy eigenstates and then evolving the state in time, as in the previous section.

a. Waveguide QED

The overall time dependence of the state when the atom is initially excited is given in Eq. (A82). The left-moving photonic wave form is therefore given by

$$\phi_L(x,t) = \langle 0|c_L(x)a_1|\psi(t)\rangle e^{i\omega_1 t} \tag{A104}$$

$$= \frac{1}{2\pi v_g}\int d\omega\, e_2^*(\omega)e^{-i\omega t}e^{-i\omega x/v_g+i\varphi}\{t_2\theta[-(x+d)] + t_1(\theta[x+d]-\theta[x])\}. \tag{A105}$$

Taking "emitted" photonic modes as those to the left of the atom, one has

$$\phi_{\rm out}(x,t) = \phi_L(x<-d,t). \tag{A106}$$

The photonic output is then

$$\phi_{\rm out}(t+x/v_g) = \frac{e^{i\varphi}}{2\pi v_g}\int d\omega\, e^{-i\omega(t+x/v_g)}e_2^*(\omega)t_2(\omega) \tag{A107}$$

$$= \frac{e^{i\varphi}}{2\pi v_g}\int d\omega\, e^{-i\omega(t+x/v_g)}\frac{\sqrt{v_g g_0}(1+e^{-i(2\omega T+\varphi)})e^{i\omega T}}{(\omega-\omega_{12})+ig_0(1+e^{i(2\omega T+\varphi)})}, \tag{A108}$$

which can be used to compute the emitted photonic wave forms for the waveguide QED case as presented in Sec. III C2.

b. Cavity QED

Again defining the emitted photonic modes to be left-moving modes to the left of the cavity and using the transmission and excitation amplitudes from Appendix A 4b, the emitted photonic wave form is

$$\phi_{\rm out}(t+x/v_g) = \frac{e^{i\varphi}}{2\pi v_g}\int d\omega\, e^{-i\omega(t+x/v_g)}e_2^*(\omega)t_2(\omega) \tag{A109}$$

$$= \frac{e^{i\varphi}}{2\pi v_g}\int d\omega\, e^{-i\omega(t+x/v_g)} \times \frac{g\sqrt{v_g\Gamma}(1+e^{-i(2\omega T+\varphi)})e^{i\omega T}}{(\omega-\omega_{12})[(\omega-\omega_c)+i\Gamma(1+e^{i(2\omega T+\varphi)}]-g^2}, \tag{A110}$$

which can be used to compute the emitted photonic wave forms for the cavity QED case.

[1] K. Hennessy, A. Badolato, M. Winger, D. Gerace, M. Atatüre, S. Gulde, S. Fält, E. Hu, and A. Imamoglu, Nature (London) **445**, 896 (2007).
[2] I. Fushman, D. Englund, A. Faraon, N. Stoltz, P. Petroff, and J. Vučković, Science **320**, 769 (2008).
[3] J. Q. You and F. Nori, Nature **474**, 589 (2011).
[4] A. Wallraff, D. Schuster, A. Blais, L. Frunzio, R. Huang, J. Majer, S. Kumar, S. Girvin, and R. Schoelkopf, Nature (London) **431**, 162 (2004).
[5] J. Eschner, C. Raab, F. Schmidt-Kaler, and R. Blatt, Nature (London) **413**, 495 (2001).
[6] C. J. Hood, M. S. Chapman, T. W. Lynn, and H. J. Kimble, Phys. Rev. Lett. **80**, 4157 (1998).
[7] T. Lund-Hansen, S. Stobbe, B. Julsgaard, H. Thyrrestrup, T. Sünner, M. Kamp, A. Forchel, and P. Lodahl, Phys. Rev. Lett. **101**, 113903 (2008).
[8] V. S. C. Manga Rao and S. Hughes, Phys. Rev. B **75**, 205437 (2007).
[9] J. M. Raimond, M. Brune, and S. Haroche, Rev. Mod. Phys. **73**, 565 (2001).
[10] H. Kimble, Phys. Scr. **1998**, 127 (1998).
[11] A. Imamoglu, D. D. Awschalom, G. Burkard, D. P. DiVincenzo, D. Loss, M. Sherwin, and A. Small, Phys. Rev. Lett. **83**, 4204 (1999).
[12] J.-T. Shen and S. Fan, Opt. Lett. **30**, 2001 (2005).
[13] J.-T. Shen and S. Fan, Phys. Rev. Lett. **98**, 153003 (2007).
[14] K. Birnbaum, A. Boca, R. Miller, A. Boozer, T. Northup, and H. Kimble, Nature (London) **436**, 87 (2005).
[15] P. Goy, J. M. Raimond, M. Gross, and S. Haroche, Phys. Rev. Lett. **50**, 1903 (1983).
[16] D. Pozar, *Microwave Engineering* (Wiley, New York, 1997).
[17] Y. Tanaka, J. Upham, T. Nagashima, T. Sugiya, T. Asano, and S. Noda, Nat. Mater. **6**, 862 (2007).
[18] M. E. Reimer, G. Bulgarini, N. Akopian, M. Hocevar, M. B. Bavinck, M. A. Verheijen, E. P. Bakkers, L. P. Kouwenhoven, and V. Zwiller, Nat. Commun. **3**, 737 (2012).
[19] J. Claudon, J. Bleuse, N. S. Malik, M. Bazin, P. Jaffrennou, N. Gregersen, C. Sauvan, P. Lalanne, and J.-M. Gérard, Nat. Photonics **4**, 174 (2010).
[20] K. Koshino and Y. Nakamura, New J. Phys. **14**, 043005 (2012).
[21] U. Dorner and P. Zoller, Phys. Rev. A **66**, 023816 (2002).
[22] Y. Chen, M. Wubs, J. Mørk, and A. F. Koenderink, New J. Phys. **13**, 103010 (2011).
[23] M. Keller, B. Lange, K. Hayasaka, W. Lange, and H. Walther, Nature (London) **431**, 1075 (2004).
[24] P. Kolchin, C. Belthangady, S. Du, G. Y. Yin, and S. E. Harris, Phys. Rev. Lett. **101**, 103601 (2008).
[25] M. Scully and M. Zubairy, *Quantum Optics* (Cambridge University Press, Cambridge, UK, 1997).
[26] R. Loudon, *The Quantum Theory of Light* (Oxford University Press, New York, 2000).
[27] M. Bradford and J.-T. Shen (unpublished).
[28] T. Yamamoto, K. Inomata, M. Watanabe, K. Matsuba, T. Miyazaki, W. D. Oliver, Y. Nakamura, and J. S. Tsai, Appl. Phys. Lett. **93**, 042510 (2008).
[29] E. Palik, *Handbook of Optical Constants of Solids* (Academic, New York, 1998).
[30] T. Erdogan, J. Lightwave Technol. **15**, 1277 (1997).
[31] H. Soekmadji, S. Liao, and R. Vernon, Prog. Electromagn. Res. Lett. **12**, 79 (2009).
[32] T. Giamarchi, *Quantum Physics in One Dimension* (Oxford University Press, New York, 2004).
[33] S. Y. Cho, H.-Q. Zhou, and R. H. McKenzie, Phys. Rev. B **68**, 125327 (2003).

[34] R. M. Konik, H. Saleur, and A. W. W. Ludwig, Phys. Rev. Lett. **87**, 236801 (2001).
[35] J.-T. Shen and S. Fan, Phys. Rev. A **79**, 023837 (2009).
[36] M. Bradford and J.-T. Shen, Phys. Rev. A **85**, 043814 (2012).
[37] R. Bose, D. Sridharan, G. S. Solomon, and E. Waks, Opt. Express **19**, 5398 (2011).
[38] H. Takano, Y. Akahane, T. Asano, and S. Noda, Appl. Phys. Lett. **84**, 2226 (2004).